Silicene multilayers on Ag(111) display a cubic diamondlike structure and a $\sqrt{3} \times \sqrt{3}$ reconstruction induced by surfactant Ag atoms

Yves Borensztein,[*] Alberto Curcella, Sébastien Royer, and Geoffroy Prévot[†]
Sorbonne Universités, UPMC Univ Paris 06, CNRS-UMR 7588, Institut des NanoSciences de Paris, 4 place Jussieu F-75005, Paris, France
(Received 27 July 2015; revised manuscript received 8 September 2015; published 6 October 2015)

The structure of silicene multilayers grown on Ag(111) and the nature of their $\sqrt{3} \times \sqrt{3}\,R30^{\circ}$ reconstruction were studied by low-energy electron diffraction, Auger spectroscopy, and optical reflectance methods. It is shown that the surface reconstruction is induced by a surfactant layer of silver atoms during the growth of the silicon film and is not due to pristine Si. The Si film displays the optical characteristics of bulk cubic diamondlike Si, which indicates that it is not formed by any other allotropic phase of Si, which does not exist in nature, whether it is stacking of silicene layers, or "silicite."

DOI: 10.1103/PhysRevB.92.155407 PACS number(s): 68.35.B−, 68.65.−k, 78.67.−n, 78.68.+m

Recent years have shown an increasing interest in two-dimensional atomic layers, like graphene, metal dichalcogenides, or boron nitrides, which display very peculiar and promising properties [1,2]. It has been shown theoretically that a self-standing single layer of silicene, the graphene counterpart for silicon, is a stable structure [3–5], and experimental investigations have proposed that silicene could be grown on different substrates: Ag(111) [6–8], Ag(110) [9], $ZrB_2(0001)$ [10,11], Ir(111) [12], and MoS_2 [13]. With electronic and transport properties similar to graphene ones, it should be more easily integrable in Si-based devices [8,9,14–16]. Most investigations have been done with Ag substrates. However, large interaction occurs between the silicene layer and the Ag substrate [17–23], leading to strong hybridization of the Ag and of the silicene states [24–27]. Decoupling the silicene layer from the substrate would be necessary for preserving its electronic properties, as shown very recently with the first silicene-based transistor obtained by removing the silicene layer from the Ag substrate [16]. Another way to achieve this decoupling would be to grow silicene multilayers, in analogy with stacked graphene multilayers. Several publications have reported the formation of bilayers and multilayers of silicene grown on Ag(111) [28–34]. Their interlayer distance, equal to 0.311 nm, is slightly smaller than the one of cubic diamondlike Si (cdSi), (0.314 nm), and they display a Raman spectrum different from the one of cdSi [33]. These silicene multilayers appear also to remain stable with time in vacuum and in air [33,35]. Theoretical models have been proposed to account for such multilayers, with different stackings of the silicene layers [36–38] or with a new structure named "silicite" [39]. With a stacking different from that of cdSi [33,39], such silicene multilayers would be the prototype of a new artificial material, that does not exist in nature. The effective elaboration of artificial silicite, similar to graphite, would therefore be a major advance in materials science, with possible novel electronic properties, and could open the way for promising applications in Si-based nanotechnology. However, the interpretation of the structural nature of the silicene multilayer has been questioned [40,41].

Bilayers and multilayers on Ag(111) display a $(4/\sqrt{3}\times4/\sqrt{3}R30^{\circ})$ surface reconstruction with respect to Ag(111), or $(\sqrt{3} \times \sqrt{3}R30^{\circ})$ reconstruction with respect to Si(111) (hereafter referred to as $\sqrt{3}$) [28–34]. Whereas it has been claimed that this reconstruction is specific to the silicene stacked film [28,30,32,42] or to the silicite structure proposed by Cahangirov *et al.* [39,43], as it has never been observed on the pristine (111) surface of cdSi, other groups have proposed that the $\sqrt{3}$ reconstruction is induced by Ag segregation at the Si surface, as the STM images are identical to the ones of the well-studied Si(111)$\sqrt{3} \times \sqrt{3}$ − Ag surface [40]. This model also fits quantitative low-energy electron diffraction (LEED) measurements performed on a 4-ML (monolayer) silicene film grown on a (111) Ag film [41].

In this article, we present a combined investigation by spot profile analysis (SPA)-LEED, Auger electron spectroscopy (AES), and optical spectroscopies, of Si multilayers deposited on the Ag(111) surface. By probing both the surface and the bulk of the layers, we solve the controversy concerning the actual nature of the silicene multilayer and of the $\sqrt{3}$ reconstruction [37]. Quantitative analysis of the Auger spectra shows that the $\sqrt{3}$ reconstructed surface is actually induced by the presence of about a half monolayer of Ag at the surface. From differential reflectance (DR) and thermoreflectance (TR) spectroscopies, which are directly linked to the optical interband transitions of the material [44–46], we elucidate the crystalline structure of the Si multilayer, and we demonstrate without ambiguity that it is not a new allotropic phase of silicon, whether it is stacking of silicene layers or silicite, but that it is bulk cubic diamondlike silicon.

Experiments have been performed in a UHV chamber with 10^{-10} mbar pressure. The Ag(111) sample was cleaned by a series of cycles of Ar ion sputtering at 0.6 keV followed by annealing at 850 K. Si was evaporated at a rate of 0.02 monolayer/min from a Si wafer piece heated by direct current. Here, one monolayer (ML) refers to the honeycomb Si(111) ML, whose density is 15.7 atom nm^{-2}. The coverage has been calibrated from the breaks observed in the AES and the DR curves at the completion of the silicene monolayer (see Supplemental Material for the determination of 1 ML from DR measurement [47]). Auger peak-to-peak intensities were measured during growth with a cylindrical mirror analyzer Auger spectrometer working at 3 keV primary beam, 45° incidence, and using a lock-in amplifier at 1 kHz with 0.4 V modulation

[*]yves.borensztein@insp.jussieu.fr
[†]geoffroy.prevot@insp.jussieu.fr

 ©2015 American Physical Society

amplitude. The optical measurements were performed with a Maya spectrometer from Ocean Optics. The DR, the relative change of reflectance of the sample caused by the Si deposit, is defined by $\mathrm{DR} = (R_{\mathrm{Si/Ag}} - R_{\mathrm{Ag}})/R_{\mathrm{Ag}}$, where R_{Ag} and $R_{\mathrm{Si/Ag}}$ are the optical reflectances of the clean and the Si-covered Ag sample measured in normal incidence. The DR was measured during Si evaporation, at a rate of one spectrum every 40 s. The TR is given by $\mathrm{TR}(T) = [R(T + \delta T) - R(T)]/R(T)$, where T is the temperature, δT an increase of temperature, and $R(T)$ the reflectance of the sample. LEED patterns were obtained with an Omicron SPA-LEED apparatus. TR and LEED measurements were performed after deposition.

Ag *MNN* and Si *LVV* transitions at 355 and 90 eV, respectively, were followed during growth at different substrate temperatures. In the following, all intensities have been normalized to the Ag intensity measured for the clean surface prior to evaporation. The evolution of the normalized Auger intensities I_{Ag} and I_{Si} for $T = 473$ K and for $T = 200$ K is shown in Fig. 1(a). For growth at 200 K, I_{Ag} decays exponentially to zero which indicates that the Si film completely covers the substrate. The Si intensity converges to $I_{\mathrm{Si}}^{\infty} = 0.74 \pm 0.04$, corresponding thus to the value expected for a clean Si surface.

For deposition at high temperature, I_{Ag} does not decay down to zero. It converges to $I_{\mathrm{Ag}}^{\infty}(473\,\mathrm{K}) = 0.13 \pm 0.01$ or $I_{\mathrm{Ag}}^{\infty}(503\,\mathrm{K}) = 0.15 \pm 0.01$. Simultaneously, the intensities $I_{\mathrm{Si}}^{\infty}(473\,\mathrm{K}) = 0.44 \pm 0.04$ and $I_{\mathrm{Si}}^{\infty}(503\,\mathrm{K}) = 0.41 \pm 0.04$ are nearly half the value measured at 200 K. Hence the thick Si films grown at high temperature do not correspond to the pure Si homogeneous film obtained at 200 K; some Ag atoms remain close to the surface.

Two explanations can be proposed. Either the surface is not homogeneously covered by Si, or Ag acts as a surfactant and remains at the surface. The first hypothesis has been proposed by De Padova *et al.* [32], but was ruled out by further x-ray diffraction measurements [33]. It can also be rejected from the LEED analysis. For both deposits, LEED diagrams acquired at the end of growth display patterns characteristic of the $\sqrt{3}$ reconstruction of Si with a main orientation at 30° and a minor orientation at 0° with respect to the Ag substrate. The LEED diagram acquired with 80-eV electrons after 10 ML evaporation at $T = 503$ K is shown in Fig. 1(b). No spots

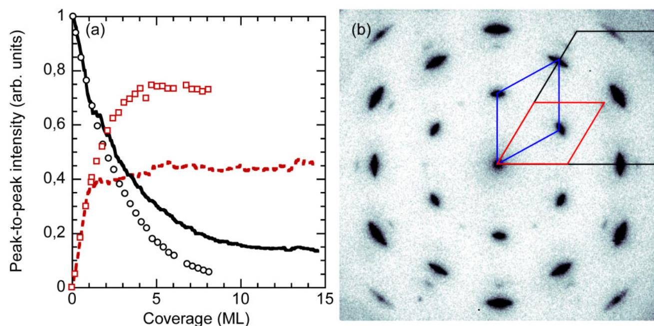

FIG. 1. (Color online) (a) Evolution of the normalized intensities of the Ag *MNN* (black continuous line/dots) and Si *LVV* (red dotted line/squares) Auger transitions during growth at 200 K (symbols) and 473 K (lines). (b) LEED diagram for 10 ML grown at 503 K ($E = 80$ eV) Unit cells of Ag(111) and Si(111)$-\sqrt{3}$ domains are drawn in black, blue, and red, respectively.

corresponding to the silicene monolayer superstructures are visible and the (1×1) substrate spots are faintly detectable. Their intensity is six orders of magnitude smaller than the value measured for the bare Ag surface.

This shows that Ag acts as a surfactant and that the Ag intensity measured in the limit of infinitely thick deposits comes from the surfactant layer. This hypothesis has been recently raised [40,41] and is also supported by the observation of the surfactant effect of Ag during Si homoepitaxy on a Si(111) substrate terminated by the $\sqrt{3} \times \sqrt{3}$ induced by 0.5 ML of Ag, at $T = 570$ K [48]. We determined the Ag quantity θ_{Ag} remaining at the surface, by using the electron effective attenuation length values at 90 eV (Si) and 355 eV (Ag) through a Ag film (0.35 and 0.55 nm, respectively [49]), taking into account the 45° analysis geometry. It can be estimated either directly from the value of $I_{\mathrm{Ag}}^{\infty}(T)$ or from the comparison of $I_{\mathrm{Si}}^{\infty}(T)$ as compared to the value obtained at $T = 200$ K. Details are given in the Supplemental Material [47].

The former estimations give θ_{Ag} equal to 0.25 ± 0.02 ML at 473 K and 0.29 ± 0.02 ML at 503 K. The latter estimations give 0.48 ± 0.1 ML and 0.54 ± 0.1 ML. The difference between the two sets of values may be explained by the uncertainties related to the determination of the Auger intensity from the peak-to-peak amplitude in the derivative of the signal, and from the estimation of the electron attenuation length for a very small thickness. These results are comparable with the coverage of the Si(111)$\sqrt{3} \times \sqrt{3}$−Ag reconstruction, i.e., 0.5 ML. Note that the value $I_{\mathrm{Ag}}^{\infty}/I_{\mathrm{Si}}^{\infty}(503\,\mathrm{K}) = 0.37$ is not far from the one measured on a Ag single layer on Si(111) (0.4) after annealing a Ag deposit at 700 K [50]; the attenuation of the Si signal as compared to the value obtained for bulk Si grown at 200 K, $I_{\mathrm{Si}}^{\infty}(503\,\mathrm{K})/I_{\mathrm{Si}}^{\infty}(200\,\mathrm{K}) = 0.55$, is also similar to the one obtained after evaporation of 0.5 ML Ag at 673 K (0.57) [51]. Thus both Auger spectra and LEED diagrams are in good agreement with a Si film covered by Ag which forms the $(\sqrt{3} \times \sqrt{3})$ reconstruction.

DR spectroscopy is an efficient optical tool for investigating adsorption processes [52–56] and thin-film growths [57,58], and has been used previously for studying Si nanoribbons on Ag(110) [59]. The DR has been measured for increasing Si amounts on the Ag(111) substrate at 479 K. Figure 2 shows the experimental spectrum obtained for the thicker Si film, about 2.1 nm, i.e., 6.7 MLs. The derivativelike negative/positive feature around 3.8 eV is due to the small reflectance of the Ag substrate at this energy, which appears in the denominator of the DR expression. However, below 3.6 eV, the reflectance of the Ag substrate is flat [60] and the features observed in this so-called Drude region originate from the silicon layer. The most relevant feature is the negative signal between 2 and 3.6 eV, in particular the shoulder at 3.3 eV (arrow).

To determine the structure of this Si film, we compare in Fig. 2 the experimental spectrum with theoretical spectra calculated for a 2.1-nm film with the dielectric functions of cdSi, silicene stacking, silicite, and amorphous Si (a-Si). The dielectric functions for Ag [61], cdSi [62], and a-Si [63] have been taken from the literature. The dielectric function for a badly crystallized silicon or for very small nanocrystallites is correctly described by that of a-Si [64]; therefore the curve calculated for a-Si corresponds also to badly crystallized Si

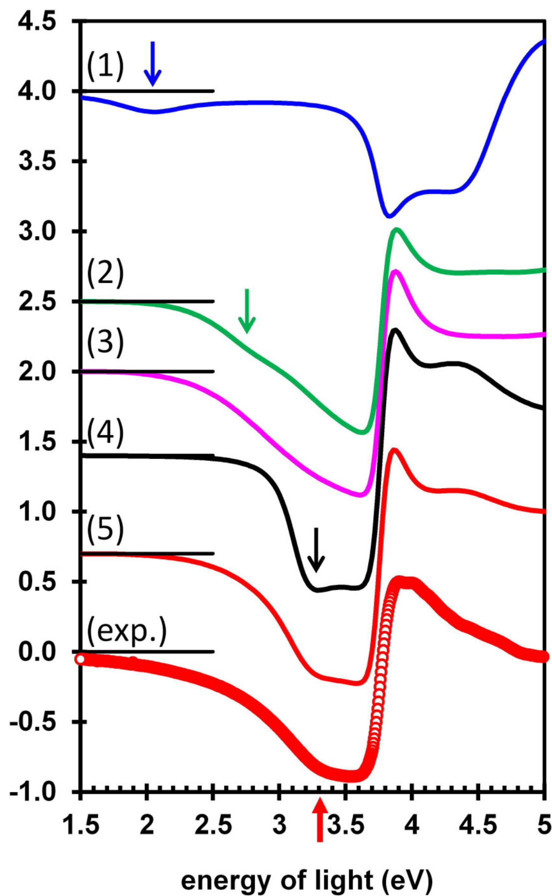

FIG. 2. (Color online) Differential reflectance spectra. Red circles: experiment. Continuous lines: calculations for different dielectric functions of the 2.1-nm silicon film. Blue (1): silicene stacking; green (2): silicite; purple (3): a-Si; black (4): cdSi; red (5): half cdSi and a-Si. The curves have been shifted upward for a better visualization.

film. In order to take into account the temperature, the Si and Ag dielectric functions have been slightly modified from the literature values given for room temperature, following Refs. [65,66]. For silicene stacking, we have considered that its optical response is the sum of the optical responses of several individual silicene layers, as shown experimentally for graphene stacking [67]; we used the dielectric function calculated by *ab initio* methods for a silicene single layer [68]. For silicite, we used the one from Ref. [39].

The spectrum for silicene stacking (1) has a completely different shape from the experimental one, and displays in particular a negative feature around 2 eV, due to an optical transition between π and π^* states. The curve obtained for a-Si (3) shows a broad negative feature between 2 and 3.6 eV, centered at 3 eV. The spectrum for silicite (2) is similar to the amorphous one, but with a slight shoulder at 2.8 eV (arrow), corresponding to a low-energy absorption line. The experimental spectrum displays no shoulder at low energy, either at 2.8 eV or at 2 eV, which seems to exclude that it is silicene stacking or silicite. On the contrary, the shape of the calculated spectrum for cdSi (4) is similar to the experimental one, with the negative shoulder at 3.3 eV (arrow) although more pronounced than in the experiment. It is directly related to the E'_o/E_1 transitions, slightly redshifted because of the temperature [65,69]. However, a thin cdSi film, even well crystallized, is not expected to get a bulklike optical response: both Si interface and surface layers interact with Ag and would have a different optical response. Consequently, the sharp negative shoulder calculated at 3.3 eV for bulk cdSi should be damped in the actual sample, as observed. We also calculated the spectrum considering that the film is only partially cdSi (half cdSi and half a-Si), drawn in Fig. 2. It is in excellent agreement with the experimental spectrum. At this point, we can therefore conclude from the present analysis that the 6.7-ML Si multilayer is correctly reproduced by an average of badly crystallized Si or a-Si, and of cdSi, but not by silicene stacking nor by silicite.

In thermoreflectance, the interband transitions are still more clearly visualized. Even if only a part of the film is cdSi, the critical points of bulk Si are expected to be present in the TR spectra. Figure 3 gives the experimental TR of the clean Ag

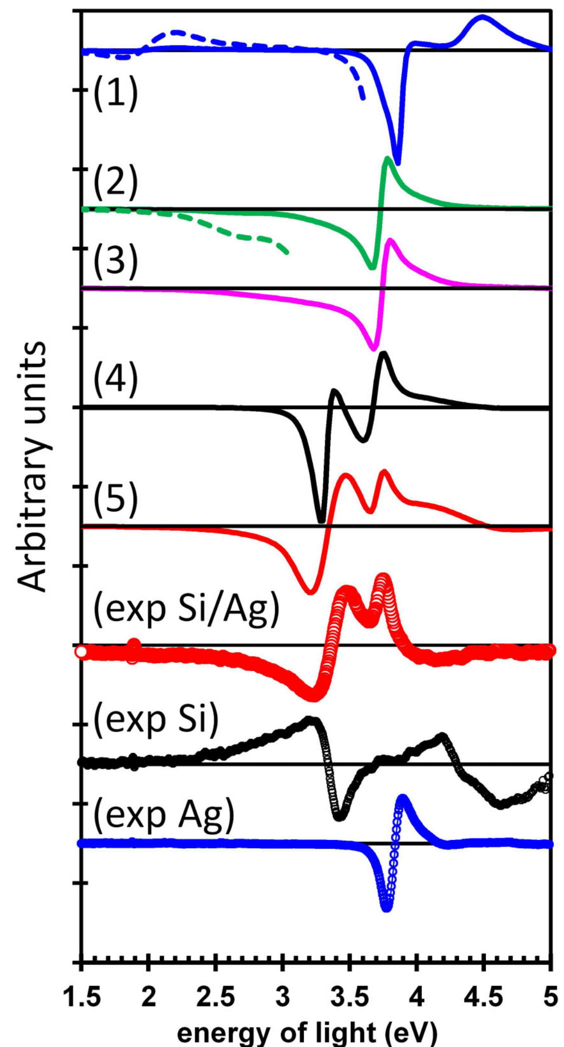

FIG. 3. (Color online) Thermoreflectance spectra. Circles: experiments; red: 2.1-nm Si/Ag; black: bulk Si; blue: bulk Ag. Continuous lines: calculations for different dielectric functions of the 2.1-nm silicon film on Ag (same as in Fig. 2). For spectra (1) and (2), the dashed lines are the spectra amplified by a factor of 7. The curves have been shifted vertically for a better visualization.

substrate, of bulk Si single crystal, and of Ag covered by the final 6.7 Si ML film. The TR for Ag and Si are identical to previously published spectra [44,70] and are explained by the redshift and broadening of the interband transitions, caused by the increase of temperature [65,66,69,71]. The TR spectrum for the 6.7-ML film displays the same derivativelike feature at 3.35 eV as for bulk Si, related to the E'_o/E_1 interband critical points in Si [65,69], but with a reverse sign (whose origin is explained in the Supplemental Material [47]). It displays also a negative/positive feature around 3.5–3.8 eV, shifted by 0.2 eV with respect to the feature measured for bulk Ag; this feature is related to the Ag substrate also probed by light across the Si film. The similarity of the TR for the Si film and for cdSi below 3.6 eV is strong evidence that the Si film is essentially constituted by cdSi.

We tentatively reproduced the TR spectra by considering simple calculations, where the dielectric functions of the materials have been rigidly redshifted, using the energy shifts experimentally determined [66,69]. Details are given in the Supplemental Material [47], where Si and Ag calculated TR are also presented to show that this approach yields good results [47]. Figure 3 gives the result when the 2.1-nm Si film is described by cdSi, by silicene stacking, by silicite, and by a-Si. The spectrum for cdSi (4) displays features at the same energies as the experimental one, although with different relative intensities. On the contrary, in the case of silicite (2) and of a-Si (3) films, the spectra resemble more that of pure Ag. In the former case, only a small bump is present around 2.8 eV. As for the silicene stacking (1), the shape of the spectrum is very far from the experimental one, and a derivative-shape feature is located around 2 eV. The positions of these features are far from the experimental ones. We finally consider, as above, a film composed by half cdSi and half a-Si. Here, we also took into account the difference in thermal expansions of Si and Ag, which are directly related to the TR. The linear thermal dilatation of Ag is $19 \times 10^{-6}\,\mathrm{K}^{-1}$, seven times larger than the one of Si which is $2.6 \times 10^{-6}\,\mathrm{K}^{-1}$ [72]. As the Si layer grows in epitaxy on Ag (with ratio of 4/3), the thermal dilatation of the Si layer is expected to be increased because of the induced stress, so the TR is in the same proportion. Hence, the TR curve for this film was calculated with a shift in energy for the dielectric function of Si seven times larger than for Ag. The result drawn in Fig. 3 is in excellent agreement with the experimental curve: This shows that the Si film has the same crystalline structure as bulk cdSi.

In conclusion, by combining Auger, LEED, and optical spectroscopies, we demonstrated that Si multilayers grown on Ag(111) at high temperatures do not form a new allotropic phase of silicon, as previously claimed, either silicene stacking or silicite, but are simply formed by cubic diamondlike silicon. The $\sqrt{3}$ reconstruction is induced by about 0.5 ML of Ag remaining at the surface. This shows that, upon the single layer of silicene grown on Ag(111), which is supposed to display a sp^3-sp^2 hybridization, additional deposited Si atoms tend to form sp^3 bonding, eventually yielding the formation of bulk cdSi film.

ACKNOWLEDGMENTS

This work was supported by French state funds managed by the ANR within the Investissements d'Avenir program under Reference ANR-11-IDEX-0004-02 and more specifically within the framework of the Cluster of Excellence MATISSE.

[1] A. K. Geim and I. V. Grigorieva, Nature **499**, 419 (2013).

[2] S. Z. Butler, S. M. Hollen, L. Cao, Y. Cui, J. A. Gupta, H. R. Gutiérrez, T. F. Heinz, S. S. Hong, J. Huang, A. F. Ismach, E. Johnston-Halperin, M. Kuno, V. V. Plashnitsa, R. D. Robinson, R. S. Ruoff, S. Salahuddin, J. Shan, L. Shi, M. G. Spencer, M. Terrones *et al.*, ACS Nano **7**, 2898 (2013).

[3] K. Takeda and K. Shiraishi, Phys. Rev. B **50**, 14916 (1994).

[4] G. Guzmán-Verri and L. C. Lew Yan Voon, Phys. Rev. B **76**, 075131 (2007).

[5] S. Cahangirov, M. Topsakal, E. Aktürk, H. Şahin, and S. Ciraci, Phys. Rev. Lett. **102**, 236804 (2009).

[6] B. Lalmi, H. Oughaddou, H. Enriquez, A. Kara, S. Vizzini, B. Ealet, and B. Aufray, Appl. Phys. Lett. **97**, 223109 (2010).

[7] P. Vogt, P. De Padova, C. Quaresima, J. Avila, E. Frantzeskakis, M. C. Asensio, A. Resta, B. Ealet, and G. Le Lay, Phys. Rev. Lett. **108**, 155501 (2012).

[8] M. Houssa, A. Dimoulas, and A. Molle, J. Phys. Condens. Matter **27**, 253002 (2015).

[9] H. Oughaddou, H. Enriquez, M. R. Tchalala, H. Yildirim, A. J. Mayne, A. Bendounan, G. Dujardin, M. Ait Ali, and A. Kara, Prog. Surf. Sci. **90**, 46 (2015).

[10] A. Fleurence, R. Friedlein, T. Ozaki, H. Kawai, Y. Wang, and Y. Yamada-Takamura, Phys. Rev. Lett. **108**, 245501 (2012).

[11] Y. Yamada-Takamura and R. Friedlein, Sci. Technol. Adv. Mater. **15**, 064404 (2014).

[12] L. Meng, Y. Wang, L. Zhang, S. Du, R. Wu, L. Li, Y. Zhang, G. Li, H. Zhou, W. A. Hofer, and H.-J. Gao, Nano Lett. **13**, 685 (2013).

[13] D. Chiappe, E. Scalise, E. Cinquanta, C. Grazianetti, B. van den Broek, M. Fanciulli, M. Houssa, and A. Molle, Adv. Mater. **26**, 2096 (2014).

[14] L. C. Yan Voon and G. G. Guzmán-Verri, MRS Bull. **39**, 366 (2014).

[15] W.-F. Tsai, C.-Y. Huang, T.-R. Chang, H. Lin, H.-T. Jeng, and A. Bansil, Nat. Commun. **4**, 1500 (2013).

[16] L. Tao, E. Cinquanta, D. Chiappe, C. Grazianetti, M. Fanciulli, M. Dubey, A. Molle, and D. Akinwande, Nat. Nanotechnol. **10**, 227 (2015).

[17] R. Bernard, T. Leoni, A. Wilson, T. Lelaidier, H. Sahaf, E. Moyen, L. Assaud, L. Santinacci, F. Leroy, F. Cheynis, A. Ranguis, H. Jamgotchian, C. Becker, Y. Borensztein, M. Hanbücken, G. Prévot, and L. Masson, Phys. Rev. B **88**, 121411(R) (2013).

[18] G. Prévot, R. Bernard, H. Cruguel, and Y. Borensztein, Appl. Phys. Lett. **105**, 213106 (2014).

[19] R. Bernard, Y. Borensztein, H. Cruguel, M. Lazzeri, and G. Prévot, Phys. Rev. B **92**, 045415 (2015).

[20] A. Resta, T. Leoni, C. Barth, A. Ranguis, C. Becker, T. Bruhn, P. Vogt, and G. Le Lay, Sci. Rep. **3**, 2399 (2013).

[21] J. Sone, T. Yamagami, Y. Aoki, K. Nakatsuji, and H. Hirayama, New J. Phys. **16**, 095004 (2014).
[22] F. Ronci, G. Serrano, P. Gori, A. Cricenti, and S. Colonna, Phys. Rev. B **89**, 115437 (2014).
[23] M. Satta, S. Colonna, R. Flammini, A. Cricenti, and F. Ronci, Phys. Rev. Lett. **115**, 026102 (2015).
[24] Z.-X. Guo, S. Furuya, J.-i Iwata, and A. Oshiyama, Phys. Rev. B **87**, 235435 (2013).
[25] Y.-P. Wang and H.-P. Cheng, Phys. Rev. B **87**, 245430 (2013).
[26] S. Cahangirov, M. Audiffred, P. Tang, A. Iacomino, W. Duan, G. Merino, and A. Rubio, Phys. Rev. B **88**, 035432 (2013).
[27] P. Gori, O. Pulci, F. Ronci, S. Colonna, and F. Bechstedt, J. Appl. Phys. **114**, 113710 (2013).
[28] B. Feng, Z. Ding, S. Meng, Y. Yao, X. He, P. Cheng, L. Chen, and K. Wu, Nano Lett. **12**, 3507 (2012).
[29] R. Arafune, C.-L. Lin, K. Kawahara, N. Tsukahara, E. Minamitani, Y. Kim, N. Takagi, and M. Kawai, Surf. Sci. **608**, 297 (2013).
[30] P. Vogt, P. Capiod, M. Berthe, A. Resta, P. De Padova, T. Bruhn, G. Le Lay, and B. Grandidier, Appl. Phys. Lett. **104**, 021602 (2014).
[31] E. Salomon, R. E. Ajjouri, G. L. Lay, and T. Angot, J. Phys.: Condens. Matter **26**, 185003 (2014).
[32] P. De Padova, P. Vogt, A. Resta, J. Avila, I. Razado-Colambo, C. Quaresima, C. Ottaviani, B. Olivieri, T. Bruhn, T. Hirahara, T. Shirai, S. Hasegawa, M. C. Asensio, and G. Le Lay, Appl. Phys. Lett. **102**, 163106 (2013).
[33] P. De Padova, C. Ottaviani, C. Quaresima, B. Olivieri, P. Imperatori, E. Salomon, T. Angot, L. Quagliano, C. Romano, A. Vona, M. Muniz-Miranda, A. Generosi, B. Paci, and G. Le Lay, 2D Mater. **1**, 021003 (2014).
[34] P. De Padova, J. Avila, A. Resta, I. Razado-Colambo, C. Quaresima, C. Ottaviani, B. Olivieri, T. Bruhn, P. Vogt, M. C. Asensio, and G. Le Lay, J. Phys.: Condens. Matter **25**, 382202 (2013).
[35] L. Donaldson, Mater. Today **17**, 370 (2014).
[36] P. Pflugradt, L. Matthes, and F. Bechstedt, Phys. Rev. B **89**, 205428 (2014).
[37] Z.-X. Guo and A. Oshiyama, New J. Phys. **17**, 045028 (2015).
[38] Z.-X. Guo and A. Oshiyama, Phys. Rev. B **89**, 155418 (2014).
[39] S. Cahangirov, V. O. Özçelik, A. Rubio, and S. Ciraci, Phys. Rev. B **90**, 085426 (2014).
[40] A. J. Mannix, B. Kiraly, B. L. Fisher, M. C. Hersam, and N. P. Guisinger, ACS Nano **8**, 7538 (2014).
[41] T. Shirai, T. Shirasawa, T. Hirahara, N. Fukui, T. Takahashi, and S. Hasegawa, Phys. Rev. B **89**, 241403 (2014).
[42] R. Arafune, C.-L. Lin, R. Nagao, M. Kawai, and N. Takagi, Phys. Rev. Lett. **110**, 229701 (2013).
[43] S. Cahangirov, V. O. Özçelik, L. Xian, J. Avila, S. Cho, M. C. Asensio, S. Ciraci, and A. Rubio, Phys. Rev. B **90**, 035448 (2014).
[44] E. Matatagui, A. G. Thompson, and M. Cardona, Phys. Rev. **176**, 950 (1968).
[45] R. Rosei and D. W. Lynch, Phys. Rev. B **5**, 3883 (1972).
[46] Y. Borensztein, Surf. Rev. Lett. **07**, 399 (2000).
[47] See Supplemental Material at http://link.aps.org/supplemental/10.1103/PhysRevB.92.155407 for additional AES results and for details of calculation.
[48] T. Yamagami, J. Sone, K. Nakatsuji, and H. Hirayama, Appl. Phys. Lett. **105**, 151603 (2014).
[49] NIST Standard Reference Database 82, NIST Electron Effective-Attenuation-Length Database; http://www.nist.gov/srd/nist82.cfm.
[50] S. Kohmoto and A. Ichimiya, Appl. Surf. Sci. **33**, 45 (1988).
[51] G. Lelay, M. Manneville, and R. Kern, Surf. Sci. **72**, 405 (1978).
[52] C. Beitia, W. Preyss, R. DelSole, and Y. Borensztein, Phys. Rev. B **56**, R4371 (1997).
[53] Y. Borensztein and N. Witkowski, J. Phys.: Condens. Matter **16**, S4301 (2004).
[54] N. Witkowski, O. Pluchery, and Y. Borensztein, Phys. Rev. B **72**, 075354 (2005).
[55] Y. Borensztein, O. Pluchery, and N. Witkowski, Phys. Rev. Lett. **95**, 117402 (2005).
[56] M. Marsili, N. Witkowski, O. Pulci, O. Pluchery, P. L. Silvestrelli, R. Del Sole, and Y. Borensztein, Phys. Rev. B **77**, 125337 (2008).
[57] Y. Borensztein, T. Lopez-Rios, and G. Vuye, Phys. Rev. B **37**, 6235 (1988).
[58] R. Lazzari, J. Jupille, and Y. Borensztein, Appl. Surf. Sci. **142**, 451 (1999).
[59] Y. Borensztein, G. Prévot, and L. Masson, Phys. Rev. B **89**, 245410 (2014).
[60] H. Ehrenreich and H. R. Philipp, Phys. Rev. **128**, 1622 (1962).
[61] P. B. Johnson and R.-W. Christy, Phys. Rev. B **6**, 4370 (1972).
[62] D. E. Aspnes and A. A. Studna, Phys. Rev. B **27**, 985 (1983).
[63] D. E. Aspnes, A. A. Studna, and E. Kinsbron, Phys. Rev. B **29**, 768 (1984).
[64] M. Losurdo, M. M. Giangregorio, P. Capezzuto, G. Bruno, M. F. Cerqueira, E. Alves, and M. Stepikhova, Appl. Phys. Lett. **82**, 2993 (2003).
[65] P. Lautenschlager, M. Garriga, L. Vina, and M. Cardona, Phys. Rev. B **36**, 4821 (1987).
[66] P. Winsemius, F. F. Van Kampen, H. P. Lengkeek, and C. G. Van Went, J. Phys. F: Met. Phys. **6**, 1583 (1976).
[67] K. F. Mak, J. Shan, and T. F. Heinz, Phys. Rev. Lett. **106**, 046401 (2011).
[68] L. Matthes, O. Pulci, and F. Bechstedt, J. Phys.: Condens. Matter **25**, 395305 (2013).
[69] G. E. Jellison, Appl. Phys. Lett. **41**, 180 (1982).
[70] E. Colavita, S. Modesti, and R. Rosei, Phys. Rev. B **14**, 3415 (1976).
[71] R. Lässer, N. V. Smith, and R. L. Benbow, Phys. Rev. B **24**, 1895 (1981).
[72] http://www.webelements.com/periodicity/coeff_thermal_expansion/.